

Measurement of Neutron Activation Cross Sections in the ${}^7\text{Li}(p,n){}^7\text{Be}$ Monoenergetic Neutron Field for Neutron Energy Range of 15 MeV to 40 MeV

著者	Titik S. S., Uwamino Y., Nakamura T.
journal or publication title	CYRIC annual report
volume	1992
page range	203-206
year	1992
URL	http://hdl.handle.net/10097/49727

V. 1. Measurement of Neutron Activation Cross Sections in the ${}^7\text{Li}(p,n){}^7\text{Be}$ Monoenergetic Neutron Field for Neutron Energy Range of 15 MeV to 40 MeV.

Titik S. S., Uwamino Y., and Nakamura T.*

*Cyclotron and Radioisotope Center, Tohoku University
Institute for Nuclear Study, University of Tokyo

Introduction

Neutron activation cross section data for neutron energy above 20 MeV are very scarce¹⁻³⁾ and discrepant and no evaluated data files are currently available. In order to fulfill this data need for dosimetry, radiation safety and material damage studies, we have estimated neutron activation cross sections for fifteen isotopes of natural and enriched samples in the energy range of 15 to 40 MeV.

The intense neutron field for sample irradiation has ever been developed using the semi-monoenergetic neutrons produced by the ${}^9\text{Be}(p,n){}^9\text{B}$ reaction^{4,5)}. The neutron spectrum was however rather broad monoenergetic peak, which required the unfolding technique to get the excitation functions. We therefore developed more monoenergetic neutron field produced by ${}^7\text{Li}(p,n){}^7\text{Be}$ reaction⁶⁾. This aimed to avoid the ambiguity coming from the unfolding method.

Samples were irradiated in the ${}^7\text{Li}(p,n)$ neutron field at the SF cyclotron of Institute for Nuclear Study (INS), while the neutron spectrum was measured with the TOF method at the AVF cyclotron of CYRIC, Tohoku University. The neutron fluence during irradiation at INS was obtained by connecting the yield of ${}^7\text{Be}$ produced in the target to the measured neutron spectrum at CYRIC via the angular-differential cross sections^{7,8)}. For these irradiations, two types of targets were employed, 2 mm thick of 99.98 % enriched ${}^7\text{Li}$ target backed with 12 mm thick carbon, as a proton beam stopper, and the only 12 mm thick carbon target.

The cross sections at the peak neutron energy, E_{peak} were estimated by taking into account the low-energy component of neutron spectrum, as the following formula :

$$\sigma(E_{\text{peak}}) = \frac{A - \int_{E_{\text{th}}}^{E_1} \sigma(E) \Phi(E) dE}{N \Phi(E_{\text{peak}})}, \quad (1)$$

where A is the reaction rate, $\Phi(E)$ the neutron spectrum, $\sigma(E)$ the neutron cross section, E_{th} the threshold energy for neutron reaction, and E_1 the minimum energy at the peak of neutron spectrum.

Experiment

Neutron spectra produced from the two targets were measured with a liquid scintillation detector NE 213 of 127 mm diam. \times 127 mm long which was placed at about 12 m behind the target. The protons of 20, 25, 30, 35 and 40 MeV bombarded these two targets at 0 deg, and the angular distributions of produced neutrons were measured using the beam-swinger system from 0 to 125 deg.

The enriched samples of ^{24}Mg , ^{25}Mg , ^{28}Si , ^{29}Si , ^{54}Fe , ^{56}Fe , ^{63}Cu , ^{65}Cu , ^{64}Zn , and ^{66}Zn , and natural samples of ^{12}C , ^{23}Na , ^{27}Al , ^{55}Mn , and ^{197}Au were activated by the $^7\text{Li}(p,n)$ neutrons produced by protons of 20, 25, 30, 35, and 40 MeV. The activities of irradiated samples were measured with the HP Ge detector. The gamma-ray peak counts were analyzed with the KEI-11EF⁹⁾ and corrected to the sum-coincidence effect and self-absorption effect¹⁰⁾.

Results

The neutron energy spectrum measured for 40 MeV proton bombardment is shown in Fig.1, for the two types of $^7\text{Li}+\text{C}$ and C targets. The dominant peak of $^7\text{Li}(p,n)^7\text{Be}$ at the neutron energy of 38 MeV comes from the ground state and the first excited state (0.429 MeV) that can not be separated due to 1.2 MeV energy loss in the target of 40 MeV proton energy. Smaller peak at 33 MeV neutron energy corresponds to the second excited state (4.57 MeV). The low-energy continuous spectrum corresponds to the higher energy state of ^7Be , and the $^{12}\text{C}(p,n)$ and $^{13}\text{C}(p,n)$ neutrons. The spectrum obtained from carbon backing shows the sharp decrease at neutron energy around 22 MeV, due to the Q-value of $^{12}\text{C}(p,n)$, -18.1 MeV.

As examples, Figures 2, 3 and 4 show the neutron activation cross sections for $^{12}\text{C}(n,2n)^{11}\text{C}$, $^{23}\text{Na}(n,2n)^{22}\text{Na}$ and $^{197}\text{Au}(n,2n)^{194}\text{Au}$ reactions, respectively. The present results of $^{12}\text{C}(n,2n)$ cross section show good agreement with the data obtained by Brill et al.¹¹⁾, except for result at 38 MeV neutron energy. The same tendency is seen in Fig.3 for $^{23}\text{Na}(n,2n)$ cross section in the present data. The result of $^{197}\text{Au}(n,4n)^{194}\text{Au}$ cross section lies in between the data by Uwamino et al.⁵⁾, and calculated data by Greenwood¹²⁾.

References

- 1) McLane V. et al., BNL-NCS-17541 (1988).
- 2) Handbook on Nuclear Activation Data, Tech. Rep. Series No. 273, IAEA (1987).
- 3) ENDF B-VI, National Cross Section Center, BNL (1990).
- 4) Uwamino Y. et al., Nucl. Sci. and Eng. 111 (1992) 391.

- 5) Uwamino Y. et al., Nucl. Inst. and Meth. **A271** (1988) 546.
- 6) Soewarsono T. S. et al., JAERI-M 92-027 (1992) 354.
- 7) Schery S. D. et al., Nucl. Inst. and Meth. **147** (1977) 399.
- 8) Orihara H. et al, Nucl. Inst. and Meth. **A257** (1987) 189.
- 9) Komura K., Inst. for Nuclear Study Report INS-TCH-7, Univ. of Tokyo, 1972.
- 10) Nakamura T., Nucl. Inst. and Meth. **105** (1972) 77.
- 11) Brill O. D. et al, DOK 136, Inst. Atom. En. I. V. Kurchatova, Moscow (1961) 55.
- 12) Greenwood L. R., ANL/FPP/TM-115, Argonne Nat. Lab., 1978.

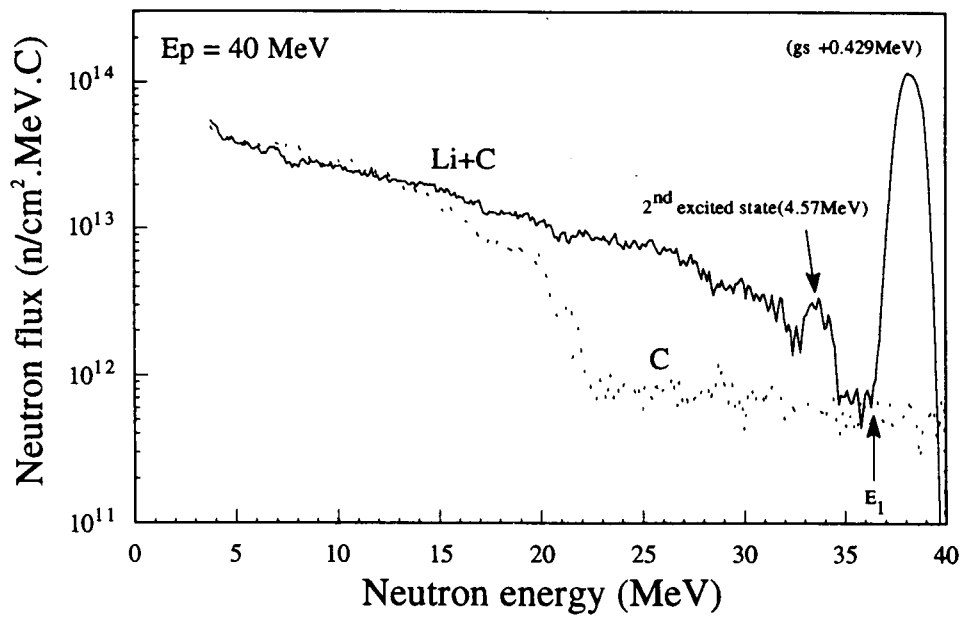


Fig. 1. Normalized neutron energy spectra of Li backed with carbon and the only carbon target for proton energy of 40 MeV.

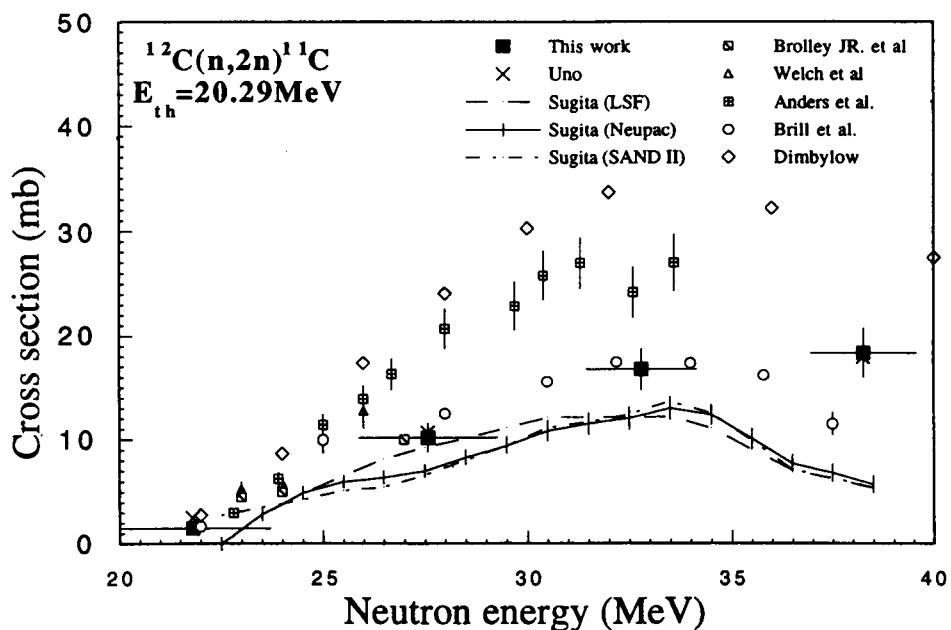


Fig. 2. Neutron activation cross sections of $^{12}\text{C}(n,2n)^{11}\text{C}$.

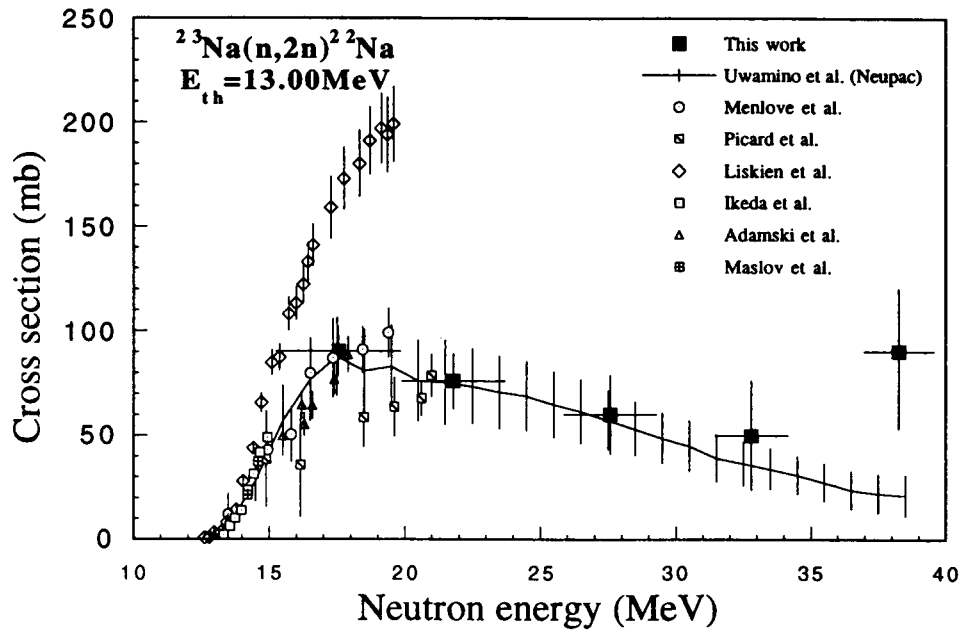


Fig. 3. Neutron activation cross sections of $^{23}\text{Na}(n,2n)^{22}\text{Na}$.

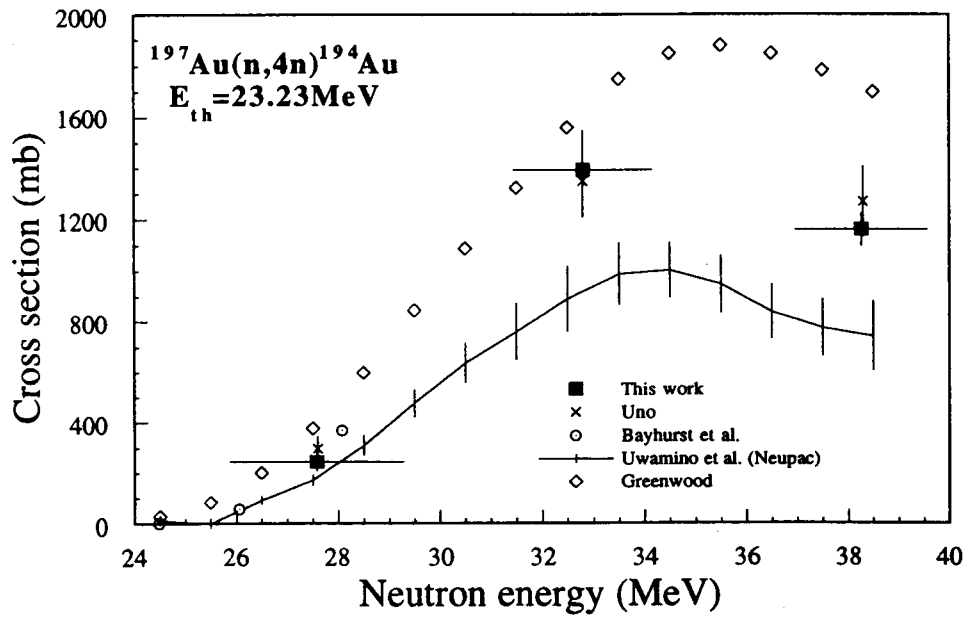


Fig. 4. Neutron activation cross sections of $^{197}\text{Au}(n,4n)^{194}\text{Au}$.